Program Development for Vibration Performance Evaluation of Powder Transfer Equipment

Hyoung-Woo Lee[1], Jeong-Hyeon Ryu[1,#] and Noh-Gill Park[2]

1 Research Institute of Mechanical Technology, Pusan University, Busan, Korea
2 Department of Mechanical Engineering, Pusan University, Busan, Korea
Corresponding Author / E-mail: 8jhryu@gmail.com, TEL: +82-51-510-1475, FAX: +82-51-514-7640

KEYWORDS : Powder transfer equipment, Decoupling, Pitching motion, Vibration, Fatigue destruction

A vibrational model of powder transfer equipment based on the lumped parameter method was developed, in which the operating motion consists of surging, bouncing, and pitching. After decoupling the equation of motion, the vibrational excitation source of the pitching motion was removed. So the designers are able to plan the optimum design to adjust the motion trajectory of the powder transfer equipment. That is, a procedure to adjust the motion trajectory of powder transfer equipment by changing design specifications such as the installation position, the direction of the motor, the driving speed, the mass unbalance, the stiffness coefficient, and the installation position of the support spring, is presented in this paper. The powder transfer equipment manufactured according to the results of this study did not suffer fatigue destruction, since the maximum stress on the basket structure was sufficiently small.

Manuscript received: August 8, 2005 / Accepted: November 8, 2005

NOMENCLATURE

ω = rotational speed of motor
e = eccentricity from the center of gravity
K = stiffness of the coil spring supporting
M = overall mass of the system with granular material
G = center of gravity
J_G = mass moment of inertia about the center of gravity
θ_x = pitching angle
F_0 = force excitation by vibrational motor
α = angle between the motor arrangement and the horizontal direction
U_{eq} = equivalent unbalance at motor
ψ = inclined angle of ellipse locus
B = semimajor axis of ellipse locus

1. Introduction

Granular materials are treated and used in many fields of industry to produce steel, chemicals, ceramics or food. The flow of these various 'powders' through industrial processes is controlled by the transfer system. Design and Construction of the transfer system requires consideration of fluidity, humidity, temperature, the size of granule and adhesiveness. Existing transfer equipment works by diverse driving mechanisms such as belt, screw[1], chain, reciprocating or vibrational motors. These days, the vibrational motor mechanism, which is more compatible with small-scale applications, is used widely due to lower noise and ease of volume control.

To design an appropriate function of powder transfer equipment with a vibrational motor mechanism within given operating conditions, it is necessary to evaluate the vibrational performance of the powder transfer equipment and the features of granular material inside. But the studies of design considering the vibrational motion are insufficient, since most concerns have been about trouble shooting.[2] In this paper, we developed a design method and program regarding the vibrational properties of powder transfer equipment. The method enables adjustment of the vibrational motion locus by decoupling the equations of motion and eliminating the vibrational source of pitching motion.

2. Vibrational model of powder transfer equipment

Fig. 1 shows the vibrational model as a lumped mass system of powder transfer equipment of which a basket structure is supported by four coil springs. The basket of the model is supposed as rigid body because the stiffness of vertical direction of the basket is much larger than that of a spring.[3~5] The installed motor with eccentric mass forces the basket structure and causes surging, bouncing, and pitching motions. The resultant of these motions moves the granular material in the basket. The drying process can be appended, if required, by blowing hot air during transfer. The governing factors of the basket vibration are the eccentric mass, the speed of the motor, the stiffness of the spring supporting, and the mass inertia of the basket with the granular material, which determine the final performance of the powder transfer equipment

2.1 Equation of Motion

In Fig. 2, K_h and K_v designate the directional components of the horizontal and vertical stiffness by spring.

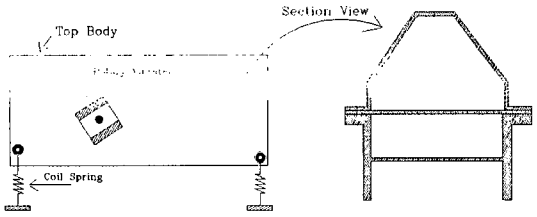

Fig. 1 Machinery component and cross section of the basket vibrator

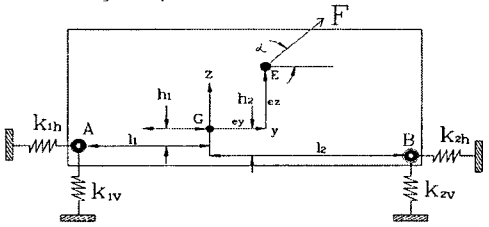

Fig. 2 Mathematical modeling of the basket vibrator

Subscripts 1 and 2 denote the components at points A and B respectively. At point E, the eccentric mass of the unbalanced motor acts in intervals of e_y, e_z around the center of gravity, point G. To describe the motions of the powder transfer equipment, a Cartesian coordinate system set up at point G, the coordinates y, z and θ_x, refer to the direction of surging, of bouncing, and of pitching, respectively. The general coordinates of the powder transfer equipment $\mathbf{q}$ denotes as follow.

$$\mathbf{q} = [y, z, \theta_x]^T$$

The equation of motion can be expressed as

$$\begin{bmatrix} M & 0 & 0 \\ 0 & M & 0 \\ 0 & 0 & J_G \end{bmatrix} \begin{Bmatrix} \ddot{y} \\ \ddot{z} \\ \ddot{\theta}_x \end{Bmatrix} + \begin{bmatrix} K_{11} & 0 & K_{13} \\ 0 & K_{22} & K_{23} \\ K_{31} & K_{32} & K_{33} \end{bmatrix} \begin{Bmatrix} y \\ z \\ \theta_x \end{Bmatrix} = \begin{Bmatrix} F_0 \cos\alpha \sin\omega t \\ F_0 \sin\alpha \sin\omega t \\ (e_y \sin\alpha - e_z \cos\alpha) F_0 \sin\omega t \end{Bmatrix} \tag{1}$$

where,

$$\begin{aligned} K_{11} &= k_{1h} + k_{2h} \\ K_{13} &= k_{1h}h_1 + k_{2h}h_2 \\ K_{22} &= k_{1v} + k_{2v} \\ K_{23} &= -k_{1v}l_1 + k_{2v}l_2 \\ K_{31} &= k_{1h}h_1 + k_{2h}h_2 \\ K_{32} &= -k_{1v}l_1 + k_{2v}l_2 \\ K_{33} &= k_{1h}h_1^2 + k_{2h}h_2^2 + k_{1v}l_1^2 + k_{2v}l_2^2 \end{aligned}$$

2.2 Design method for improving vibrational performance

2.2.1 Requirement for the locus of the basket

To move the granular material uniformly, the basket must maintain horizontality and the regular locus of ellipse during operation. Therefore, the pitching motion should be eliminated, since the inclination and the major axis of the ellipse must be fixed. As a result, the basket can move through a consistent locus of inclined ellipse. To design this required specification, we had to satisfy the following two necessaries, decoupling the motion of surging, bouncing, and pitching in equation (1), and eliminating pitching excitation. Then, the required motion of the basket could be controlled by adjusting the surging and bouncing.

2.2.2 Decoupling the equation of motion and eliminating the pitching motion

The condition for decoupling equation of motion (1) is that the stiffness matrix $\mathbf{K}$ in equation (1) must be decoupled. That is,

$$k_{1h}h_1 + k_{2h}h_2 = 0 \tag{2}$$

$$-k_{1v}l_1 + k_{2v}l_2 = 0 \tag{3}$$

The equivalent moment about the center of gravity is $(e_y \sin\alpha - e_z \cos\alpha)F_0 \sin\omega t$, which excites the pitching motion. To minimize this motion, the equivalent moment must be zero: or

$$e_y \sin\alpha - e_z \cos\alpha = 0 \tag{4}$$

Equation (4) could also be expressed as follows:

$$\alpha = \tan^{-1}\left(\frac{e_z}{e_y}\right) \tag{5}$$

The mathematical model of the decoupled basket vibrator is illustrated in Fig. 3.

2.2.3 Decoupling the equation of motion and eliminating the pitching motion

Substituting equations (2), (3) and (5) into (1), the decoupled equation of motion of the powder transfer equipment yields,

$$M\ddot{y} + (k_{1h} + k_{2h})y = 2U_{eq}\omega^2 \cos\alpha \sin\omega t \tag{6}$$

$$M\ddot{z} + (k_{1v} + k_{2v})z = 2U_{eq}\omega^2 \sin\alpha \sin\omega t \tag{7}$$

$$J_G\ddot{\theta}_x + (k_{1h}h_1^2 + k_{2h}h_2^2 + k_{1v}l_1^2 + k_{1v}l_2^2)\theta_x = 0 \tag{8}$$

The natural frequencies from equations (6), (7), and (8) are

$$(\omega_n)_y = \sqrt{\frac{k_{1h} + k_{2h}}{M}} \tag{9}$$

$$(\omega_n)_z = \sqrt{\frac{k_{1v} + k_{2v}}{M}} \tag{10}$$

$$(\omega_n)_0 = \sqrt{\frac{k_{1h}h_1^2 + k_{2h}h_2^2 + k_{1v}l_1^2 + k_{2v}l_2^2}{J_G}} \tag{11}$$

Substituting $y = y_0 \sin\omega t$, $z = z_0 \sin\omega t$ into equations (6) and (7), the responses of forced vibration are

$$y = \frac{2U_{eq}\omega^2 \cos\alpha \sin\omega t}{k_{1h} + k_{2h} - M\omega^2} \tag{12}$$

$$z = \frac{2U_{eq}\omega^2 \sin\alpha \sin\omega t}{k_{1v} + k_{2v} - M\omega^2} \tag{13}$$

Equations (12) and (13) denote the reciprocating linear locus of motion, as shown in Fig. 4. The basket moves along the locus of ellipse inclined by the angle of ψ about the horizontal axis; B refers to the semimajor axis of this ellipse, as shown in Fig. 4. ψ and B can be expressed as

$$\psi = \tan^{-1}\left(\tan\alpha \frac{k_{1h} + k_{2h} - M\omega^2}{k_{1v} + k_{2v} - M\omega^2}\right) \tag{14}$$

$$B = 2U_{eq}\omega^2 \sqrt{\left(\frac{\cos\alpha}{k_{1h} + k_{2h} - M\omega^2}\right)^2 + \left(\frac{\sin\alpha}{k_{1v} + k_{2v} - M\omega^2}\right)^2} \tag{15}$$

These equations show that ψ is determined by the forcing frequency ω and the directional angle of vibrational motor α, that is,

$$\psi = \psi(\omega, \alpha) \tag{16}$$

$$B = B(\omega, \alpha, \theta) \tag{17}$$

Equations (16) and (17) could have several solutions, an easy-to-manufacture solution would be selected in design.

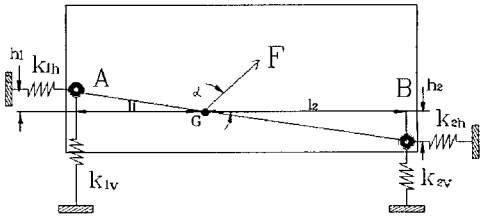

Fig. 3 Decoupled basket vibrator

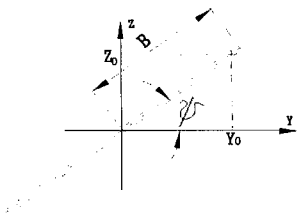

Fig. 4 Basket vibrator having sloped ellipse motion

2.2.4 Design of locus

Two procedures for designing the powder transfer mechanism are explained in the following section, where the inclination ψ and the magnitude B, the semimajor axis of elliptical locus, are given as design specifications.

2.2.4.1 Algorithm I

The method of design using the same kind of spring is as follows.

Step①: Input data determining the size of the basket structure, which are the thickness, the width, the density of the basket, the weight, the horizontal dimension of the flange, the location of the springs at both edges of the basket.

Step②: Calculate the global mass of the whole system(M), the center of gravity(G), and the mass moment of inertia about G(J_G).

Step③: Select the spring to use. Then, the stiffness of the support springs in the form of horizontal and vertical components (K_h , K_v) are computed with equations (18) and (19).

$$K_h = \frac{K_v}{1.44C_l\left(0.204\left(\frac{h_s}{D}\right)^2 + 0.265\right)} \tag{18}$$

$$K_v = \frac{G_s d^4}{8N_a D^3} \tag{19}$$

where,

N_a	number of effective winding of coil spring
G_s	coefficient of shear
D	diameter of coil spring
d	diameter of wire
h_s	length of compressed coil spring
C_l	spring deformation coefficient[7]

Step④: Determine the location of the support coil springs according to equations (2) and (3).

To install the springs parallel to the line of the center of gravity, the conditions $h_1 = h_2 = 0$, $l_1 = l_2$ can be applied. Or to allow some offset from the center of gravity, the conditions $-h_1 = h_2$, $l_1 = l_2$ will be applied.

Step⑤: Install the vibrational motor at the center of gravity(G), keeping the direction angle of vibrational motor α adjustable.

Step⑥: Determine the rotating speed of the vibrational motor ω .

Step⑦: Determine the inclination angle ψ and the magnitude B .

Step⑧: Calculate the directional angle of vibrational motor α producing the inclination angle ψ .

Step⑨: Determine the eccentric mass producing the magnitude B .

2.2.4.2 Algorithm II

The method of design using a different kind of spring is as follows.

Step①: Input data determining the size of the basket structure.

Step②: Calculate the global mass of the whole system(M), the center of gravity(G), and the mass moment of inertia about G(J_G).

Step③: Determining the location of the support springs yields the relative distance from the center of gravity to the point of support springs A, B. That is h_1 , h_2 , l_1 , l_2 are fixed.

Step④: Step ④ consists of the sub-steps ④-1 and ④-2.

④-1: Select the spring at point A and calculate the horizontal and vertical components of stiffness. Then, the specifications of the spring at point B can be determined by equations (2) and (3). That is the stiffness components K_h , K_v are

$$K_h = K_h(N_a, d, D, G_s, L_0) \tag{20}$$

$$K_v = K_v(N_a, d, D, G_s) \tag{21}$$

L_0 denotes the length of spring without deformation. The parameters N_a , d , D , and G_s can be determined by the each of the stiffness values K_h , K_v .

④-2: Select the spring at point B and calculate the horizontal and vertical components of stiffness. Then, the specifications of the spring at point A can be determined by equations (2) and (3). That is, the stiffness components K_h , K_v are determined by equations (20) and (21).

Steps⑤~⑨ are the same as those of algorithm I.

3. Design of the powder transfer equipment

The required conditions of design can be classified into 4 cases as follows.

Case I: Using the same kind of support spring parallel to the center of gravity and changing the horizontal position of point A to satisfy $l_1 = l_2$.

Case II: Using the same kind of support spring parallel to the center of gravity and changing the horizontal position of point B to satisfy $l_1 = l_2$.

Case III: Using a different kind of support spring parallel to the center of gravity and changing the specifications of the spring at point A to satisfy equation (3).

Case IV: Using a different kind of support spring parallel to the center of gravity and changing the specifications of the spring at point A to satisfy equation (4).

The design program was run under the conditions of each of the 4 cases described above. The design program determines the specifications and positions of springs that can decouple the system as well as the location to install the vibrational motor, which is the source of excitation of the pitching motion. The excitation frequency ω , the angle of installation of motor α , and the relative angle θ between the two unbalance disks can also be determined by the program when the input parameters, which are the magnitude B and the angle between the locus of the basket and horizontal direction ψ , are by the user.

3.1 Design under Case I

In case I, using the same kind of support spring parallel to the center of gravity and changing the horizontal position of point A to satisfy $l_1 = l_2$, the results are shown in Table 1. The excitation frequency ω , the angle of installation of motor α , and the relative angle θ between the two unbalance disks are solved as shown in Table 2.

The frequency response of the design according to the 1st data(ω = 17.817 rad/s, α = 64.1°, θ = 2°) in Table 2 is shown in Fig. 5, where each motion is decoupled and the magnitude of the pitching motion is zero. Fig. 6 shows the locus around the center of gravity. The points s_{ah} , s_{bh} listed in Table 1 are move on the same locus, since the pitching motion is eliminated. Fig.

7 and Fig. 8 show the stress distributions of sections s_a and s_b , where the maximum stress(0.03 MPa) is less than the fatigue strength(206.01 MPa), which indicates that the design is safe against fatigue fracture.

Table 1 Result I after processing design program

Variable	Value
Center of gravity (c_h , c_v)	c_h = 1.037 m c_v = -0.006 m
Position of fixing motor (m_h , m_v)	m_h = 1.037 m m_v = 0.006 m
Position of fixing spring A (s_{ah} , s_{av})	s_{ah} = 0.364 m s_{av} = 0.006 m
Position of fixing spring B (s_{bh} , s_{bv})	s_{bh} = 0.260 m s_{bv} = 0.006 m
ψ	30°
B	0.001 m

Table 2 Result II after processing design program

Kind	ω (rad/s)	α (deg)	θ (deg)
1	17.817	64.10	2.00
2	25.291	14.60	2.00

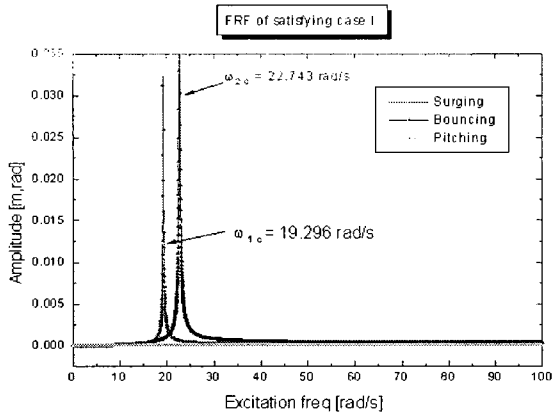

Fig. 5 Frequency response of case I

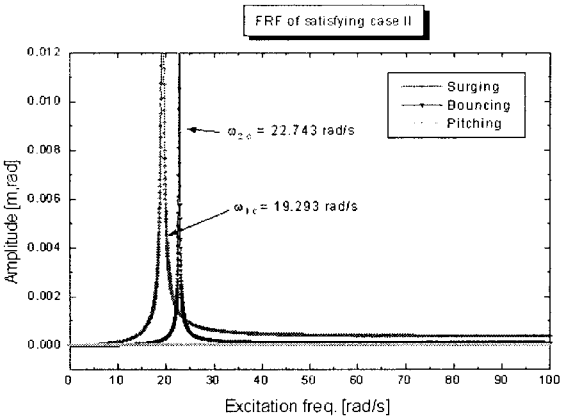

Fig. 9 Frequency response of case II

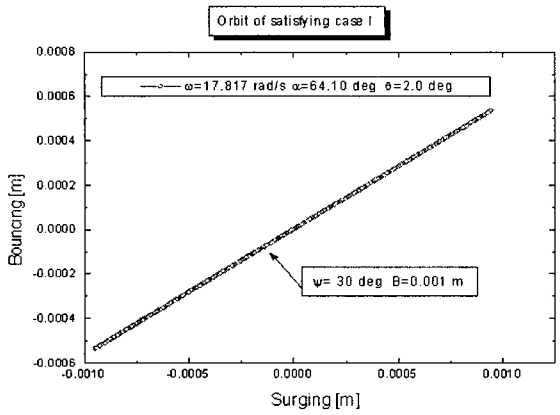

Fig. 6 Orbit at point G of case I

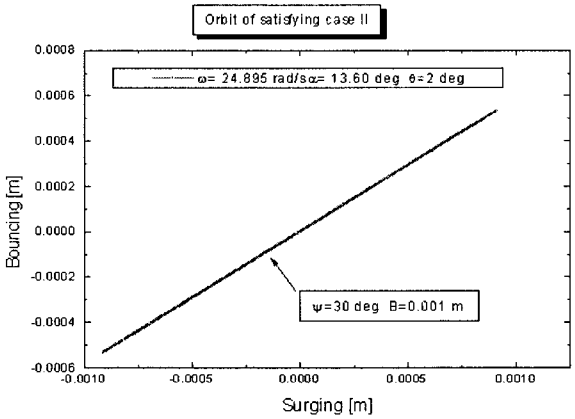

Fig. 10 Orbit at point G of case II

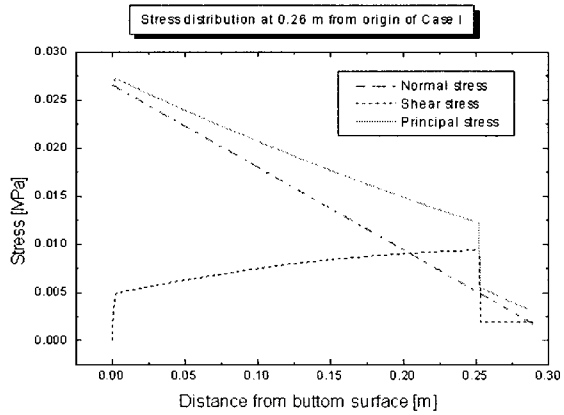

Fig. 7 Stress distribution of s_a cross section

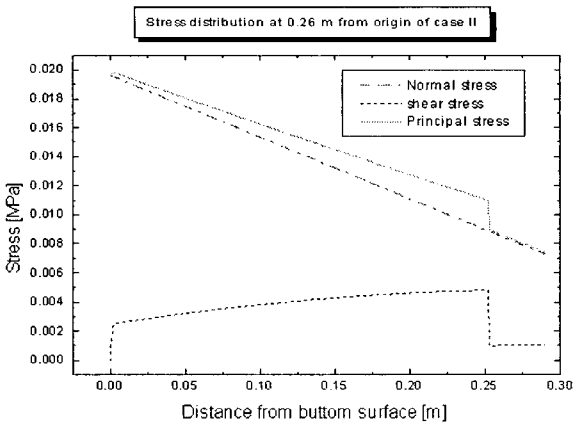

Fig. 11 Stress distribution of s_a cross section

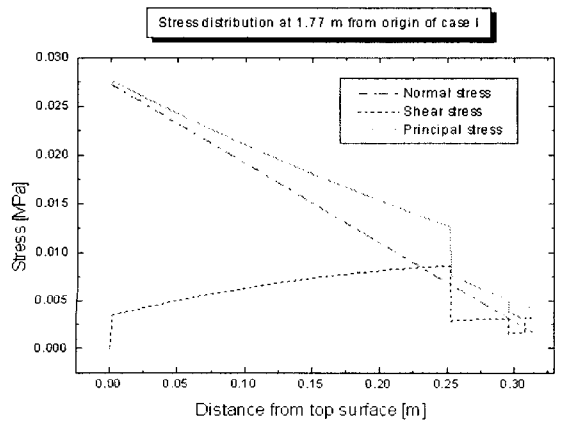

Fig. 8 Stress distribution of s_b cross section

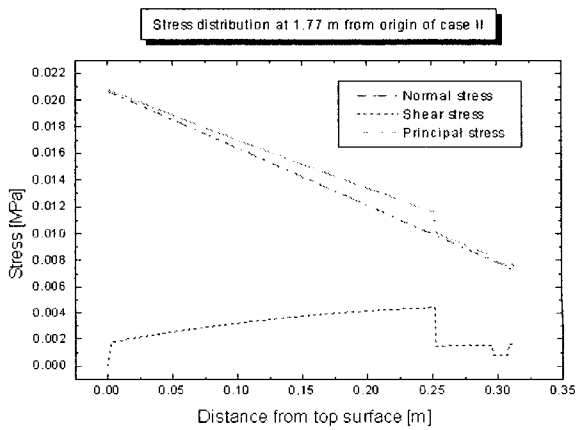

Fig. 12 Stress distribution of s_b cross section

Table 3 Result I after processing design program

Variable	Value
Center of gravity (c_h, c_v)	c_h = 1.037 m c_v = -0.006 m
Position of fixing motor (m_h, m_v)	m_h = 1.037 m m_v = 0.006 m
Position of fixing spring A (s_{ah}, s_{av})	s_{ah} = 0.320 m s_{av} = 0.006 m
Position of fixing spring B (s_{bh}, s_{bv})	s_{bh} = 0.216 m s_{bv} = 0.006 m
ψ	30°
B	0.001 m

Table 4 Result II after processing design program

Kind	ω (rad/s)	α (deg)	θ (deg)
1	18.920	81.10	2.00
2	24.895	13.60	2.00

3.2 Design under Case II

In case II, using the same kind of support spring parallel to the center of gravity and changing the horizontal position of point B to satisfy $l_1 = l_2$, the results are shown in Table 3. The excitation frequency ω, the angle of installation of motor α, and the relative angle θ between the two unbalance disks in this case are solved as shown in Table 4.

The frequency response of the design according to the 2nd data(ω = 24.895 rad/s, α = 13.6°, θ = 2°) in Table 4 is shown in Fig. 9, where each motion is decoupled and the magnitude of the pitching motion is zero. Fig. 10 shows the locus around the center of gravity. The points s_{ah}, s_{bh} listed in Table 3 move on the same locus, since the pitching motion is eliminated.

Fig. 11 and Fig. 12 show the stress distributions of sections s_a and s_b, where the maximum stress(0.02 MPa) is still less than the fatigue strength(206.01 MPa), which indicates that the design is safe against fatigue fracture.

3.3 Design under Case III and Case IV

In case III a different kind of support spring parallel to the center of gravity is used, and the specifications of the spring at point A are changed. In case IV, a different kind of support spring parallel to the center of gravity is used, and the specifications of the spring at point B are changed. The results are presented in Table 5.

The excitation frequency ω, the angle of installation of motor α, and the relative angle θ between the two unbalance disks are solved as Table 6. The frequency responses of the design in case III and case IV according to the data in Table 6 are shown in Fig. 13 and Fig. 14, respectively.

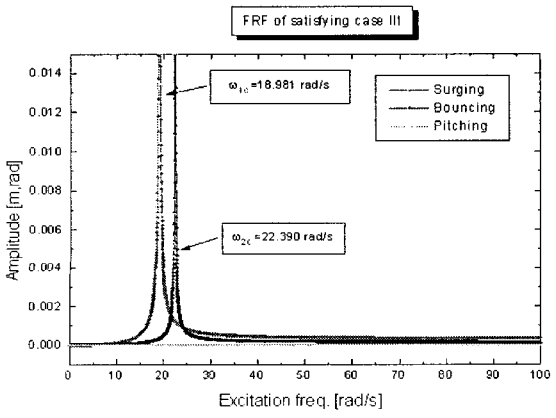

Fig. 13 Frequency response of case III

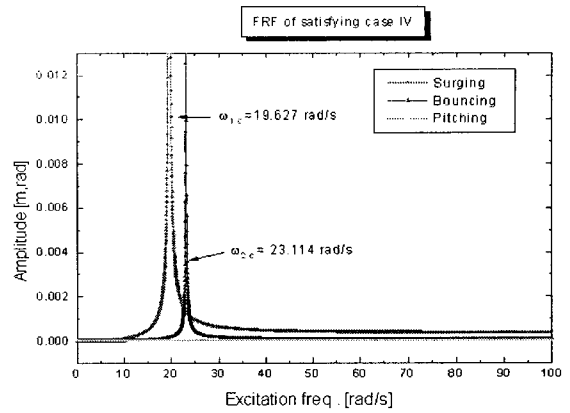

Fig. 14 Frequency response of case IV

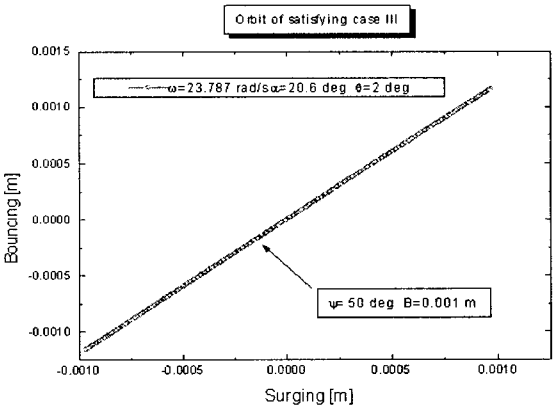

Fig. 15 Orbit at point G of case III and case IV

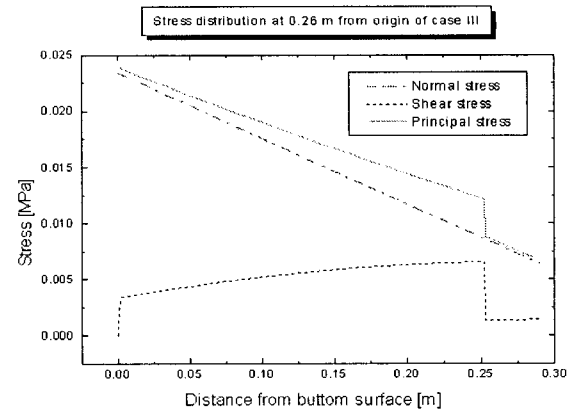

Fig. 16 Stress distribution of s_a cross section (case III)

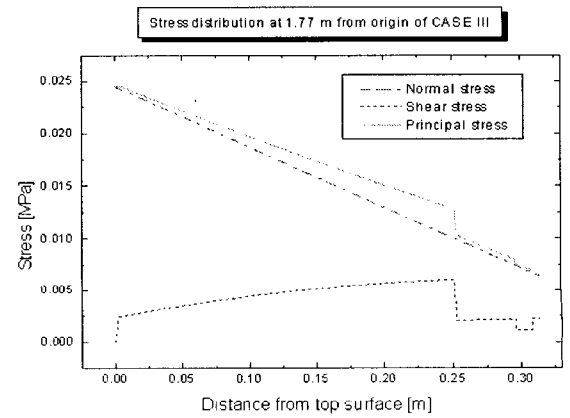

Fig. 17 Stress distribution of s_b cross section (case III)

Table 5 Results after processing design program

Variable	Value (case III)	Value (case IV)
Center of gravity (c_h , c_v)	c_h = 1.038 m, c_v = -0.006 m	c_h = 1.038 m, c_v = -0.006 m
Position of fixing motor (m_h , m_v)	m_h = 1.037 m, m_v = 0.006 m	m_h = 1.038 m, m_v = 0.006 m
D	0.112 m	0.108 m
d	0.012 m	0.012 m
N_a	7.457 turns	6.569 turns
K_v	40.976 kN/m	46.534 kN/m
K_h	29.449 kN/m	33.554 kN/m

Table 6 Results obtained after processing design program

Kind	α (deg)	θ (deg)	ω (rad/s)-case III	ω (rad/s)-case IV
1	20.60	2.00	23.787	24.524
2	32.10	2.00	25.686	26.484
3	32.60	2.00	25.686	26.484

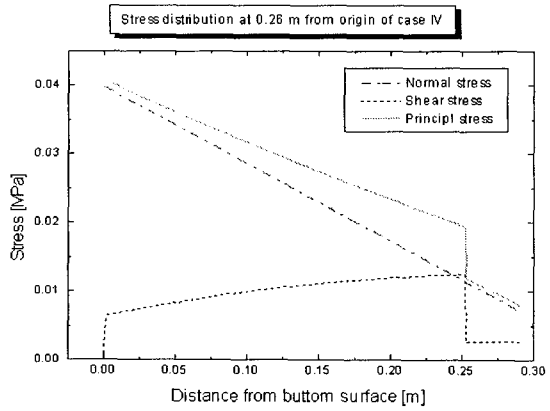

Fig. 18 Stress distribution of s_a cross section (case IV)

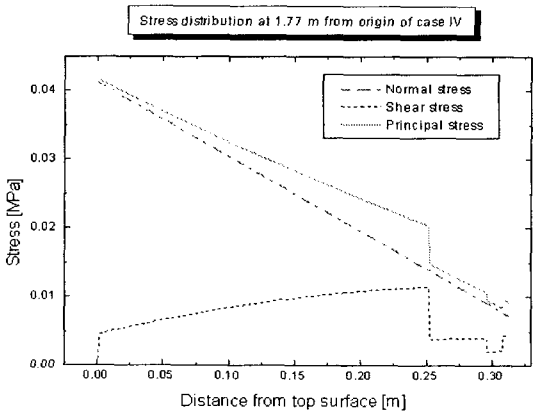

Fig. 19 Stress distribution of s_b cross section (case IV)

Fig. 15 shows the locus around the center of gravity. The points c_h , s_{ah} and s_{bh} listed in Table 5 are move on the same locus, since the pitching motion is eliminated. Fig. 16, Fig. 17, Fig. 18, and Fig. 19 show the stress distributions of sections s_a and s_b. In Fig. 16 and Fig. 17, the maximum stress is 0.07 MPa. In Fig. 18 and Fig. 19, the maximum stress is 0.04 MPa. In both cases, the maximum stress is still less than the fatigue strength(206.01 MPa), which indicates that both designs are safe against fatigue fracture.

4. Conclusions

A design method and a program regarding the vibrational properties of powder transfer equipment were developed and studied. The method enables the adjustment of the vibrational motion locus by decoupling the equations of motion and eliminating the vibrational source of pitching motion.

1. The design program was developed under 4 sets of design restrictions, aforementioned.
2. The design method to adjust the locus of the basket of the powder transfer equipment, based on decoupling the equation of motion, is presented. The locus of the basket was controlled by adjusting several parameters: the stiffness and location of the support spring, the angle and location to install the vibrational motor, the operating speed, and the mass unbalance.
3. The designs are safe from fatigue fracture, since the analyzed maximum stresses are still relatively less than the fatigue strength.

REFERENCES

1. Choi, B. H., Jeong C. K., Choi, S. H., "Tooth Shape Design for the Screw Flights Cutting in Twin Screw Extruder," Proceedings of the Korean Society of precision Engineering Conference, pp. 824-828, May 2002.
2. Shigley, J. E., Mischke, C. R., "Mechanical Engineering Design," McGraw-hill, 1989.
3. Wu, C. Y., Dihoru, L., Cocks, A. C. F., "The flow of powder into simple and stepped dies," Powder Technology, Vol. 134, pp. 24-39, 2003.
4. Jenike, A. W., "Storage and flow of solids," Bulletin, Vol.123, Engineering Experiment Station, University of Utah, 1964.
5. Tuzun, U., Heyes, D. M., "Distinct element simulations and dynamic microstructural imaging of slow shearing granular flows," Mechanics of Granular and Porous Materials, pp. 263-274, 1997.
6. Zhang, L., "Shear deformation of granular media in pure shear, direct shear and simple shear," PhD Thesis, Aston University, 2003.
7. Oda, M., Iwashita, K., "Mechanics of Granular Materials," Balkema, Rotterdam, 1999.
8. Cleary, P. W., Sawley, M. L., "DEM modeling of industrial granular flows: 3D case studies and the effect of particle shape on hopper discharge," Applied Mathematical Modeling, Vol. 26, pp. 89-111, 2002.